

MVDREAM: MULTI-VIEW DIFFUSION FOR 3D GENERATION

Yichun Shi¹, Peng Wang¹, Jianglong Ye^{2*}, Long Mai¹, Kejie Li¹, Xiao Yang¹

¹ ByteDance, USA, ² University of California, San Diego

{yichun.shi, peng.wang, kejie.li, xiao.yang}@bytedance.com

{jianglong.yeh, mai.t.long88}@gmail.com

ABSTRACT

We propose *MVDream*, a multi-view diffusion model that is able to generate geometrically consistent multi-view images from a given text prompt. By leveraging image diffusion models pre-trained on large-scale web datasets and a multi-view dataset rendered from 3D assets, the resulting multi-view diffusion model can achieve both the generalizability of 2D diffusion and the consistency of 3D data. Such a model can thus be applied as a multi-view prior for 3D generation via Score Distillation Sampling, where it greatly improves the stability of existing 2D-lifting methods by solving the 3D consistency problem. Finally, we show that the multi-view diffusion model can also be fine-tuned under a few shot setting for personalized 3D generation, i.e. DreamBooth3D application, where the consistency can be maintained after learning the subject identity. Our project page is <https://MV-Dream.github.io>

1 INTRODUCTION

3D content creation is an important step in the pipeline of modern game and media industry, yet it is a labor-intensive task that requires well-trained designers to work for hours or days to create a single 3D asset. A system that can generate 3D content in a easy way by non-professional users is thus of great value. Existing 3D object generation methods can be categorized into three types: (1) template-based generation pipeline (2) 3D generative models and (3) 2d-lifting methods. Due to limited accessible 3D models and large data complexity, both template-based generators and 3D generative models can so far hardly generalize to arbitrary object generation. Their generated content is usually limited to certain categories, which are common objects from real world with relatively simple topology and texture. Yet in real industry, popular 3D assets usually come as a mixture of complicated, artistic and sometimes non-realistic structures and styles (Ske).

Recently, 2D-lifting methods have shown that pre-trained 2D generation models can be potentially applied to 3D generation. The typical representations are Dreamfusion (Poole et al., 2023) and Magic3D (Lin et al., 2023a) systems, which utilize 2D diffusion models as supervision for the optimization of a 3D representation, such as NeRF (Mildenhall et al., 2021), via score distillation sampling (SDS). Trained on large-scale 2D image datasets, these 2D models have excellent generalizability and they are able to generate unseen and counterfactual scenes whose details can be specified through a text input, making them great tools for creating artistic 3D assets. Nevertheless, because these models only have 2D knowledge, they can only provide single-view supervision and the generated assets generated easily suffer from the multi-view consistency issue. This makes the generation rather unstable and their results often contain severe artifacts.

In 2D-lifting techniques, challenges arise due to the lack of comprehensive multi-view knowledge or 3D-awareness during score distillation. These include: (1) The multi-face Janus issue: The system frequently regenerates content described by the text prompt. (2) Content drift across different views. Examples can be seen in Fig. (1). The multi-face issue can stem from various factors. For instance, certain objects, like blades, may be nearly invisible from some angles. Meanwhile, vital parts of a character or animal might be hidden or self-occluded from certain viewpoints. While humans assess

*Work done during internship at ByteDance

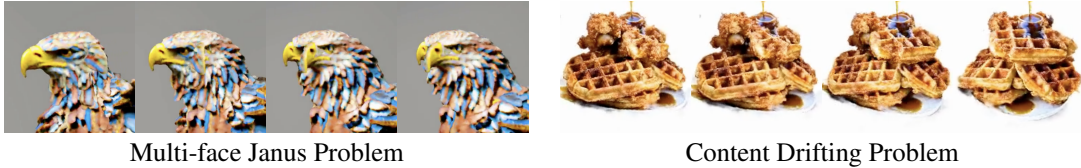


Figure 1: Typical multiview-consistency problems of 2D-lifting methods for 3D generation. Left: “A bald eagle carved out of wood” where the eagle has two faces. Right: “a DSLR photo of a plate of fried chicken and waffles with maple syrup on them” where the chicken gradually becomes a waffle.

these objects from multiple angles, a 2D diffusion model cannot, leading it to produce redundant and in-consistent content.

To overcome such problems, we propose multi-view diffusion models, which simultaneously generate a set of multi-view images that are consistent with each other. We keep the architecture design of 2D image diffusion while slightly changing it for multi-image generation. This allows us to use pre-trained 2D diffusion models for transfer learning to inherit their generalizability. To ensure the multi-view consistency of our model, we render a set of multi-view images from a real 3D dataset, namely objaverse (Deitke et al., 2023). By jointly training the model on multi-view images and real images, we find that the resulting model can achieve both a good consistency and generalizability. We further apply these models to 3D generation via multi-view score distillation. It turns out that the multi-view supervision from our model is much more stable than those of single-view 2D diffusion models. And we can still create unseen, counterfactual 3D contents as from pure 2D diffusion models. Inspired by DreamBooth (Ruiz et al., 2023) and DreamBooth3D (Raj et al., 2023), we also employ our multi-view diffusion model to assimilate identity information from a collection of provided images and it demonstrates robust multi-view consistency after such a few-show fine-tuning. When incorporated into the 3D generation pipeline, our model, namely *MVDream*, successfully generates 3D Nerf models without the Janus issue. It either surpasses or matches the diversity seen in other state-of-the-art methods.

2 RELATED WORK AND BACKGROUND

2.1 3D GENERATIVE MODELS

The significance of 3D generation has driven the application of nearly all deep generative models to this task. Handerson *et al.* explored Variational Auto Encoders (VAEs) (Kingma & Welling, 2014) for textured 3D generation (Henderson & Ferrari, 2020; Henderson et al., 2020). However, their studies mainly addressed simpler models leveraging multi-view data. With Generative Adversarial (GAN) Models yielding improved results in image synthesis, numerous studies have investigated 3D-aware GAN training from 2D data (Nguyen-Phuoc et al., 2019; 2020; Niemeyer & Geiger, 2021; Deng et al., 2022; Chan et al., 2022; Gao et al., 2022). A notable advantage of these methods, attributed to the absence of reconstruction loss involving ground-truth data in adversarial loss, is the independence from real 3D or multi-view data, allowing training solely on monocular images. Yet, akin to 2D GANs, they face challenges with generalizability and training stability for diverse object and scene generation. Consequently, diffusion models, which have shown marked advancements in general image synthesis, have become recent focal points in 3D generation studies. Depending on the chosen 3D representation, various diffusion models have been introduced, including those using Tri-plane (Shue et al., 2023; Wang et al., 2023b) or Feature grid (Karnewar et al., 2023). Nevertheless, current 3D diffusion models primarily cater to specific objects like faces and ShapeNet objects. Their generalizability to the scope of their 2D counterparts remains unverified, possibly due to 3D model constraints or architectural design. It’s pertinent to note ongoing research endeavors to reconstruct object shapes directly from monocular image inputs (Wu et al., 2023; Nichol et al., 2022; Jun & Nichol, 2023), aligning with the increasing stability of image generation techniques.

2.2 DIFFUSION MODELS FOR OBJECT NOVEL VIEW SYNTHESIS

Recent research has also pursued the direct synthesis of novel 3D views without undergoing reconstruction. For instance, Watson et al. (2023) introduced the application of diffusion models

to the ShapeNet dataset (Sitzmann et al., 2019). Zhou & Tulsiani (2023) leverages the stable diffusion model (Rombach et al., 2022) combined with an epipolar feature transformer, crafting a view-conditioned diffusion model in the latent space. Concurrently, Chan et al. (2023) seeks to enhance the view consistency of the diffusion model by reprojecting the latent features of the input view prior to diffusion denoising. A limitation shared across these approaches is their boundedness to their respective training data, with no established evidence of generalizing to diverse image inputs such as the generated ones. In contrast, Liu et al. (2023) employs a pre-trained image variation stable diffusion model (sdv), subsequently fine-tuning it on an extensive 3D render dataset. Notwithstanding, the synthesized images from such studies, exemplified by the Zero123 demo, still grapple with maintaining realistic geometric consistency, leading to a discernible blurriness in the output 3D models. Recently, Tang et al. (2023) propose a multi-view diffusion model for panorama with homography-guided attention, which is different from ours where 3D correspondence is not available.

2.3 LIFTING 2D DIFFUSION FOR 3D GENERATION

Given the difficulty of 3D generative models generalizing to unconstrained types of objects, another thread of studies have attempted to apply 2D diffusion models as a prior to 3D generation by coupling it with a 3D representation, such as a NeRF (Mildenhall et al., 2021). The key technique of such methods is the score distillation sampling (SDS) proposed by Poole et al. (2023), where the diffusion priors are used as score functions to supervise the optimization of a 3D representation. Concurrent with Dreamfusion, SJC (Wang et al., 2023a) propose a similar technique using the publicly available stable-diffusion model (sta). Following works have further improve this type of methods by improving 3D representation (Lin et al., 2023a; Tsalicoglou et al., 2023; Chen et al., 2023), sampling schedule (Huang et al., 2023) and loss design (Wang et al., 2023c). Although these methods can generate photo-realistic and arbitrary types of objects without training on any 3D data, they are known to suffer from the multi-view consistency problem, as discussed in Section 1. In addition, as discussed in (Poole et al., 2023), each generated 3D model is individually optimized by tuning prompts and hyper-parameters, e.g. camera extrinsics, to avoid generation failures. Nevertheless, in MVDream, we significantly improve the generation robustness, and are able to produce satisfactory results with a single set of parameters without individual tuning.

We further explore the concept of subject-driven 3D model creation using a collection of identification images, as introduced by DreamBooth3D (Raj et al., 2023). Their approach recommends a three-stage optimization: beginning with a partial DreamBooth model, transitioning to image-to-image translation, and culminating in training a multi-view 3D DreamBooth model. In contrast, our MVDream capitalizes on the inherent consistency of our diffusion model, streamlining the process: we commence by training a multi-view (MV) DreamBooth model followed by 3D NeRF optimization. Notably, our MVDreamBooth model achieves faster training speeds and yields 3D models of superior geometric consistency, markedly reducing Janus-related challenges.

3 METHODOLOGY

3.1 WHY MULTI-VIEW DIFFUSION?

In order to lift 2D diffusion models for 3D generation without multi-view consistency issue, a typical solution is to improve its viewpoint-awareness. For example, Poole et al. (2023) adds viewpoint descriptions into texts as conditions. A more sophisticated method would be incorporating exact camera parameters like in novel view synthesis methods (Liu et al., 2023). However, we hypothesize that even a perfect camera-conditioned model is not sufficient to solve the problem and the content in different view still could mismatch. For example, an eagle might look to its front from front view while looking at its right from back view, where only its body is complying with the camera condition.

Our next inspiration draws from video diffusion models. Since we human do not have a real 3D sensor, the typical way to perceive a 3D object is to circle around it and observe it from all possible perspectives. Such an evaluation process is similar to rendering and watching a turnaround video. Recent works on video generation demonstrate the possibility of adapting image diffusion models to generate consistent content (Ho et al., 2022; Singer et al., 2022; Blattmann et al., 2023; Zhou et al., 2022). However, adapting such video models to to our problem of multi-view generation is

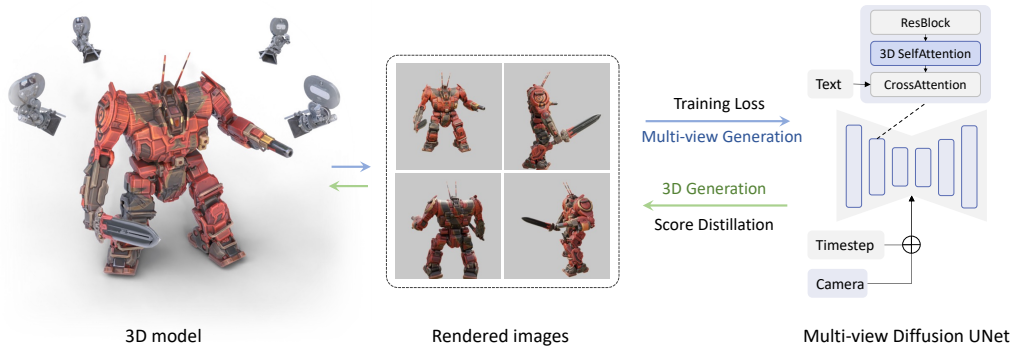


Figure 2: Illustration of the overall multi-view diffusion model. During training, multi-view images are rendered from real 3D models to train the diffusion model, where we keep the structure of the original text-to-image UNet by making two slight changes: (1) changing the self-attention block from 2D to 3D for cross-view connection (2) adding camera embeddings to the time embeddings for each view. During testing, the same pipeline is used in a reverse way. The multi-view diffusion model serves as 3D prior to optimize the 3D representation via Score Distillation Sampling (SDS).

non-trivial as geometric consistency could be more delicate than temporal consistency. Our initial experiment shows that content drifting could still happen between frames for video diffusion priors when there is a large viewpoint gap between. Moreover, video diffusion prior are usually trained on dynamic scenes, which suffer from a domain gap when working as a prior for static scenes.

With such observations, we found it important to directly train a multi-view diffusion prior for the 3D generation task, where we could utilize 3D rendered dataset to generate static scenes and have access to precise camera parameters.

3.2 TEXT-TO-MULTI-VIEW DIFFUSION MODEL

Fig. (2) shows an illustration of our text-to-multi-view diffusion model. We leverage the 3D datasets to render consistent multi-view images to supervise the diffusion model training. Formally, given a set of noisy image $\mathbf{x}_t \in \mathbb{R}^{F \times H \times W \times C}$, a text prompt as condition y , and a set of extrinsic camera parameters $\mathbf{c} \in \mathbb{R}^{F \times 16}$, multi-view diffusion model is trained to generate a set of images $\mathbf{x}_0 \in \mathbb{R}^{F \times H \times W \times C}$ of the same scene from F different view angles. After the training, the model can be used a multi-view prior for 3D generation with techniques such as Score Distillation Sampling (SDS).

In order to inherit the generalizability of the text-to-image models, we would like to keep the architecture of the 2D prior model as much as possible and fine-tune them on the text-to-multi-view task. However, the original text-to-image model can only generate one image at a time and does not take camera conditions as inputs. So the main questions here are: (1) how to generate a set of images from the same text prompt which are consistent to each other (Sec. 3.2.1), (2) how to add the camera pose control into the text-to-image model (Sec. 3.2.2), and (3) how to maintain the quality and generalizability of the original diffusion model (Sec. 3.2.3).

3.2.1 MULTI-VIEW CONSISTENT IMAGE GENERATION

Similar to video diffusion models (Ho et al., 2022; Singer et al., 2022; Blattmann et al., 2023; Zhou et al., 2022), we would like to adapt the attention layers to model the cross-view dependency while keeping the remaining network as a 2D model that only operates within a single image. However, we found that a simple temporal attention fail to learn multi-view consistency and content drifting still happens even if we fine-tune the model on a 3D rendered dataset. Instead, we choose to use a 3D attention. Specifically, we can convert original 2D self-attention layer into 3D by connecting different views in the self-attention layer (See Fig. 3). In such a way, the model would in fact generate similar images without fine-tuning. After training on multi-view datasets, such 3D attended diffusion UNet is able to generate rather consistent images even when the view gap is very large. Note that with such 3D attention, our multi-view diffusion model is permutation-invariant where the order of the

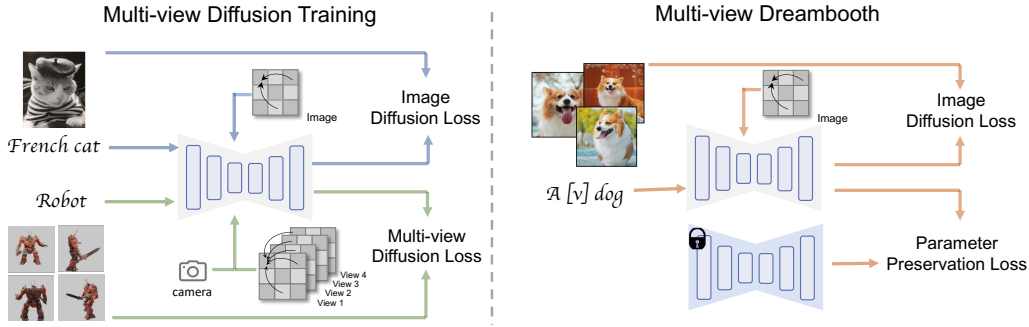


Figure 3: Illustration of the training pipeline of MVDream. Left: Training of Multi-view diffusion (MVDiffusion), it is mixed trained with two modes: with the 2D attention (upper) and 3D multi-view attention (lower). Details in Sec. 3.2.3. Right: Training of MVDreamBooth, it takes the pre-trained MVDiffusion model, and then finetuned with the mode of 2D attention and a preservation loss. Details in Sec. 3.4.

viewpoint/position conditions is no longer important like in the video diffusion models. Additionally, we experimented with incorporating a new 3D self-attention layer rather than modifying the existing one. However, this design compromised the generation quality of multi-view images. We suspect the slower convergence of a new attention module relative to re-utilizing parameters from an existing one is to blame. Given our reluctance to fine-tune the diffusion model extensively, we opted not to pursue this approach further.

3.2.2 CAMERA EMBEDDINGS

Like video diffusion models, position encoding is necessary for our model to distinguish between different views. Our initial attempt was to use the same relative position encoding (Singer et al., 2022) from video diffusion models since we believe a relative viewpoint condition is sufficient for our downstream tasks. However, it turns out that such relative position encoding is too ambiguous for our task and model often generates repeated views. On the other side, simply embedding the extrinsic camera matrix (with a 2-layer MLP) leads to more precise results, where each view is distinguishable from others.

Another question is where to inject these camera embeddings. We identify two methods: (1) adding each view’s camera embedding to its time embedding as residuals and (2) appending the camera embeddings to the text embeddings for cross attention. Our experiment shows that both methods work but the first option turns out to be more robust because the camera embeddings would be less entangled with text description.

3.2.3 DATA AND TRAINING

In spite of the access to ground-truth 3D rendered data, we found that the way of utilizing such data is still crucial to the generability and quality of the multi-view diffusion model. The key factors are concluded as follows:

1. The choice of viewpoints.
2. The number of views of generated images.
3. The resolution of generated images.
4. Joint training with original text-to-image datasets.

Specifically, we found that rendering with completely random viewpoints would lead to too much training difficulty, and the model can hardly generate descent results. Thus, for each object, we choose to only use different viewpoints uniformly distributed at the same elevation angle, which is randomly chosen between 0 and 30 degrees. As for the number of views, we found that a larger number of views also increases the convergence difficulty and therefore we choose to only use 4

views for the current models. Following Zero123 (Liu et al., 2023), we reduce the image size to 256×256 , which turns out to be quite helpful for the multi-view consistency.

For the training, we fine-tune our model from the Stable Diffusion v2.1 base model (512×512 resolution), where we keep their settings for the optimizers and ϵ -prediction. We found that a joint training with a larger scale text-to-image dataset is also helpful for the generalizability of the fine-tuned model, as illustrated in the left Fig. (3). Formally, given dataset of images \mathcal{X} and multi-view images \mathcal{X}_{mv} , for training samples $\{\mathbf{x}, y, \mathbf{c}\} \in \mathcal{X} \cup \mathcal{X}_{mv}$ the multi-view diffusion loss is defined as

$$\mathcal{L}_{MV}(\theta, \mathcal{X}, \mathcal{X}_{mv}) = \mathbb{E}_{\mathbf{x}, y, \mathbf{c}, t, \epsilon} \left[\|\epsilon - \epsilon_{\theta}(\mathbf{x}_t; y, \mathbf{c}, t)\|_2^2 \right] \quad (1)$$

where \mathbf{x}_t is the noisy image generated from ϵ and \mathbf{x}, y is the condition, \mathbf{c} is the camera condition and the ϵ_{θ} is the multi-view diffusion model. In practice, with a 30% chance we train the multi-view model as a simple 2D text-to-image model on a subset of LAION dataset (Schuhmann et al., 2022) by turning off the 3D attention and camera embeddings..

3.3 TEXT-TO-3D GENERATION

Once we have a diffusion model that generates consistent multi-view images from a text description, we recognize two ways to utilize it for 3D generation:

- Use the multi-view generated images as inputs for a few-shot 3D reconstruction method for generating 3D content
- Use the multi-view diffusion model as a prior for 3D optimization via Score Distillation Sampling (SDS).

Although the former solution is more straight forward, 3D reconstruction methods typically requires many input angles to achieve pleasant results. They would have a higher requirement of the consistency between the input images. While our diffusion model’s multi-view images appear consistent, their geometric compatibility isn’t assured.

Therefore, in this work, we mainly focus our experiments on the later choice., where we modify the existing SDS pipeline by replacing the commonly used Stable Diffusion model with our multi-view diffusion model. This only leads to two modifications. First, we change the camera sampling strategy such that every time we sample a set of uniformly distributed F view angles on the same elevation angle. Second, we feed the absolute camera extrinsic matrix as inputs to our diffusion model. Instead of using direction-annotated prompts as in Dreamfusion (Poole et al., 2023), we simply use the original text prompts for extracting the text embeddings.

Although SDS with multi-view diffusion is able to generate consistent 3D models. The content richness and texture quality of such generated models are still far from those images directly sampled by diffusion models. Thus, we propose several techniques to alleviate the issue. First, instead of sampling time step in a fixed range as in original SDS, we linearly anneal the maximum and minimum time step during optimization. Second, to prevent the model from generating styles of those low quality 3D models in the dataset, we add a few fixed negative prompts during SDS. Finally, to alleviate the color saturation from large classifier free guidance (CFG), one common option is to apply clamping methods such as dynamic thresholding (Saharia et al., 2022) or CFG rescale from (Lin et al., 2023b) to adjust the denoised $\hat{\mathbf{x}}_0$. Although these tricks only apply to $\hat{\mathbf{x}}_0$ while the original SDS is defined by ϵ_{θ} , we show that an \mathbf{x}_0 -reconstruction loss

$$\mathcal{L}_{SDS}(\phi, \mathbf{x} = g(\phi)) = \mathbb{E}_{t, \mathbf{c}, \epsilon} \left[\|\mathbf{x} - \hat{\mathbf{x}}_0\|_2^2 \right] \quad (2)$$

is equivalent to the original SDS with $w(t)$, a hyper-parameter in SDS, equal to signal-to-noise ratio (See Appendix). Here $\mathbf{x} = g(\phi)$ refer to rendered images from 3D representation ϕ and $\hat{\mathbf{x}}_0$ is the estimated \mathbf{x}_0 from $\epsilon_{\theta}(\mathbf{x}_t; y, \mathbf{c}, t)$, whose gradient is detached. Empirically we found that \mathbf{x}_0 -reconstruction loss performs similarly to original SDS but it mitigates the color saturation after we apply the CFG rescale trick (Lin et al., 2023b).

We also turn on the point lighting (Poole et al., 2023) and soft shading (Lin et al., 2023a) to regularize the geometry. For regularization loss, we only use the orientation loss proposed by (Poole et al., 2023). We note that both of these two techniques only helps to smooth the geometry and has little effect on the content in our case. We do not use any sparsity loss to force the separation between foreground the background but instead achieve it by replacing background with random colors.

3.4 MULTI-VIEW DREAMBOOTH FOR 3D GENERATION

As shown in the right of Fig. (3), once we got the pre-trained network from multi-view diffusion, we consider to extend it to a DreamBooth model (Ruiz et al., 2023) for 3D DreamBooth applications. Thanks for the generalization of multi-view diffusion model, we found its multi-view ability is able to be maintained after it is tuned. Specifically, we consider two type of loss, an image fine-tuning loss and a parameter preservation loss. Formally, let \mathcal{X}_{id} indicates the set of identity images, our loss for DreamBooth is,

$$\mathcal{L}_{DB}(\theta, \mathcal{X}_{id}) = L_{LDM}(\mathcal{X}_{id}) + \lambda \frac{\|\theta - \theta_0\|_1}{N_\theta} \quad (3)$$

where \mathcal{L}_{LDM} is the image diffusion loss (Rombach et al., 2022), θ_0 is the initial parameter of original multi-view diffusion, N_θ is the number of parameters, and λ is a balancing parameter set to 1. In practice, we train the model around 600 steps with a learning-rate as $2e - 6$, weight decay as 0.01 and a batch size of 4, yielding a good balance between identity preserving and conditioned stylization.

Finally, to obtain a 3D model, we follow the text to 3D generation process in Sec. 3.3 by replacing the diffusion model with MV DreamBooth model. After the NeRF model is trained, our results mitigate the Janus issue as observed in some results of DreamBooth3D, yet produces models with better details and quality, which are shown with Fig. 9 in our experiments.

4 IMPLEMENTATION DETAILS

4.1 DATA PREPARATION AND DIFFUSION MODEL TRAINING

We use the public Objaverse dataset (Deitke et al., 2023) as our 3D rendered dataset, which was the largest 3D dataset available by the time of this project. We simply use the name and tags of the objects as their text descriptions. Since this dataset is rather noisy, We filter the dataset with a CLIP score to remove the objects whose rendered images are not relevant to its name, which leads to about 350K objects at the end. For each object, we first normalize the object to be at the center, and then choose a random camera distance between $[0.9, 1.1]$, fov between $[15, 60]$ and elevation between $[0, 30]$. A random HDRI from blender is used for lighting. 32 uniformly distributed azimuth angles are used for rendering, starting from the front view. To increase the number of training examples, we render each object twice with different random settings.

During the training, we sample a data batch with a 70% chance from the 3D dataset and 30% chance from the aes V2 subset of LAION dataset (Schuhmann et al., 2022). For the 3D dataset, 4 random views which are orthogonal to each other is chosen from the 32 views for training. We fine-tune our model from the Stable Diffusion v2.1 base model (512×512 resolution), where we keep their settings for the optimizer and ϵ -prediction. We use a reduced image size of 256×256 and a total batch size of 1,024 (4,096 objects) for training and fine-tune model for 50,000 steps. The training takes about 3 days on 32 Nvidia Tesla A100 GPUs. To compensate for the visual style difference between Objaverse and LAION dataset, we append the text “, 3d asset” to the 3D data if the keyword “3d” is not in the prompt.

4.2 SDS OPTIMIZATION

For multi-view SDS, we implement our multi-view diffusion guidance in the threestudio (thr) library, which has implemented most state-of-the-art methods for text-to-3D generation under a unified framework. We use the implicit-volume implementation in threestudio as our 3D representation, which include a multi-resolution hash-grid and a MLP to predict density and RGB. For camera views, we sample the camera in exactly the same way as how we render the 3D dataset. See Sec. 4.1 for more details. The 3D model is optimized for 10,000 steps with an AdamW optimizer (Kingma & Ba, 2014) at a learning rate of 0.01. For SDS, the maximum and minimum time step are decreased from 0.98 to 0.5 and 0.02, respectively, over the first 8,000 steps. We use a rescale factor of 0.5 for the CFG rescale trick. The rendering resolution starts at 64×64 and is increased to 256×256 after the 5,000 steps. We also turn on soft shading as in (Lin et al., 2023a) after 5,000 steps. The background is replaced with 50% chance.

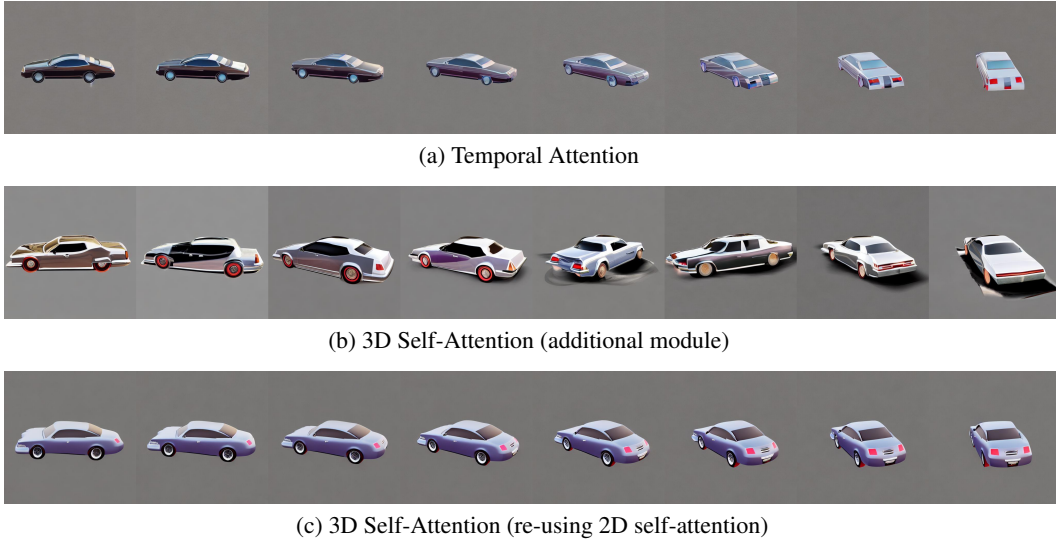


Figure 4: Effect of different attention module. Experiment conducted on a 512×512 model trained with 8 continuous azimuth angles spanning 90 degrees. Same random seed used for training and testing.

| Model | Batch Size | FID↓ | IS↑ | CLIP↑ |
|--------------------------------|------------|-------|------------------|------------------|
| training data | N/A | N/A | 14.75 ± 0.81 | 31.31 ± 3.34 |
| Multi-view Diffusion | | | | |
| - no LAION data joint training | 256 | 33.41 | 12.76 ± 0.70 | 30.60 ± 3.14 |
| - proposed | 256 | 32.57 | 13.72 ± 0.91 | 31.40 ± 3.05 |
| - proposed (larger batch size) | 1024 | 32.06 | 13.68 ± 0.41 | 31.31 ± 3.12 |

Table 1: Quantitative evaluation on image synthesis quality. All models are sampled using DDIM sampler.

5 EXPERIMENTS

5.1 MULTI-VIEW IMAGE GENERATION

In this section, we evaluate the image generation quality of the proposed multi-view diffusion model and how different design could affect the performance.

We first compare the choice of the attention module that are used to model the cross-view consistency. The options include (1) 1D temporal self-attention that are widely used in video diffusion models, (2) a new 3D self-attention module that are added onto existing model, and (3) reusing existing 2D self-attention module for 3D attention. In this experiment, to clearly visualize the difference between these modules, we trained the models with 8 frames across 90-degree view change, which is closer to a video settings. We also kept a higher image resolution at 512×512 as original SD model in this experiment.

The results are shown in Fig. (4), we found that even with such limited view angle change on static scenes, the temporal self-attention still suffers from the content shift and cannot maintain view consistency. We hypothesize that this is because the temporal attention can only interchange information between the same pixel from different frames while the corresponding pixels could be far away from each other while the view point is changing. Adding new 3D attention, on the other side, leads to severe quality degradation without learning the consistency. We believe this is because learning new parameters from scratch would take more training data and time, which is unsuitable for ours case where limited 3D models are available. The proposed strategy of re-using 2D self-attention achieves the best consistency among all without losing the generation quality. We note that the difference between these modules would be much smaller if we reduce the image size to 256 and number of views to 4. However, to achieve the best consistency, we keep our choice for the following experiments based on our initial observations.

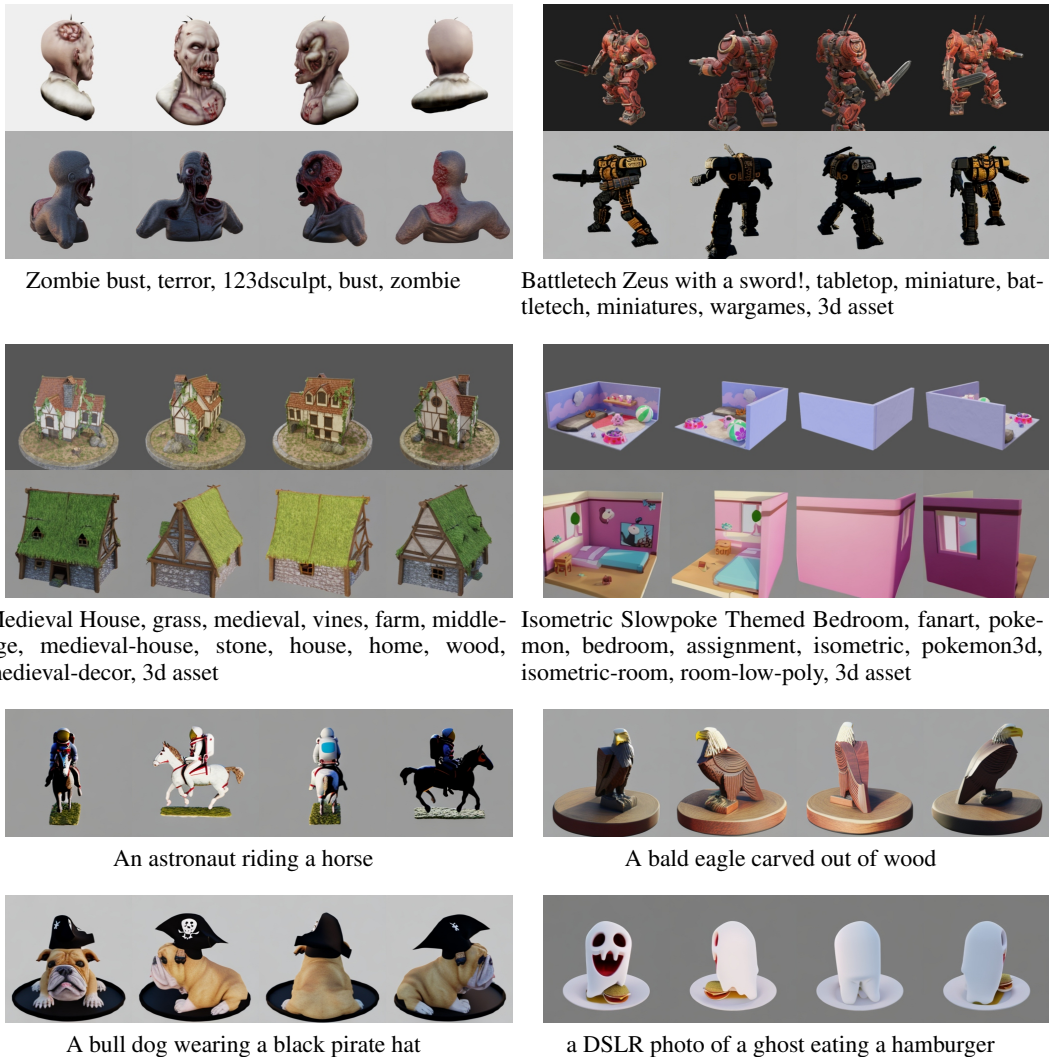


Figure 5: Example images generated by our multi-view diffusion model using prompts in training set and testing set. In top four examples, the top and bottom row are the training and generated images, respectively. The bottom four examples are images generated using unseen prompts.

In Table 1, we conduct a quantitative comparison over the generation quality and text-image consistency. In particular, we randomly choose 1,000 subjects from the training set and generate 4 multi-view images using the given prompts and camera parameters. Frechet Inception Distance (FID) (Heusel et al., 2017) and Inception Score (IS) (Salimans et al., 2016) are calculated to measure the image quality while the CLIP score (Radford et al., 2021) is used to measure the text-image consistency. Because the cameras are random, we simply average across all views and subjects to calculate the final CLIP score. Overall, our models can achieve a similar Inception Score and CLIP score as the original training set, indicating a good generation quality and text-image consistency. Adding text-to-image dataset (LAION) further improves the CLIP score and Inception score. Compared to IS score, the FID is relative large. We hypothesize that this is caused by the color difference between generated images and training samples, where our generated images tend to have less brightness change and a gray background. Increasing batch size from 256 to 1,024 does bring clear improvement in terms of quality measure, but visually we found it helpful to improve the multi-view consistency. In Fig. (5), we show a few qualitative examples from training set and our model. Overall, the multi-view diffusion model can generate good quality multi-view consistent images that match both the text description and camera parameters in a precise way.

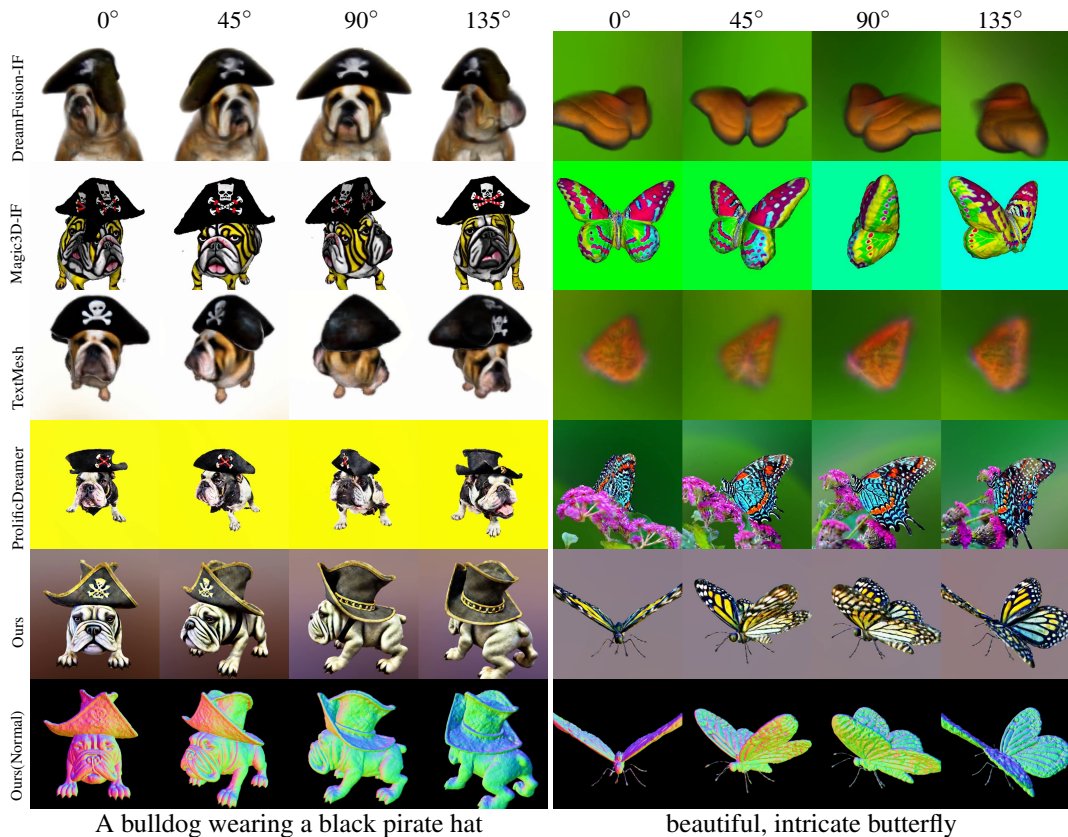


Figure 6: Comparison of text-to-3D generation between baselines and our method. See Appendix for more results.

Fig. (5) shows more examples of our multi-view model with unseen prompts that are possibly counterfactual and in a different style from training prompts. Like training, we append the text with “, 3d asset” for generation. It can be seen that the model is able to still generalize to different text inputs after the fine-tuning.

5.2 3D GENERATION WITH MULTI-VIEW SCORE DISTILLATION

In this section, we apply our multi-view diffusion model to 3D generation with SDS and compare with existing text-to-3d methods. Since we implement the SDS of our multi-view diffusion in the threestudio framework (thr), for fairness, we also use the reproduced baselines this framework for comparison. In particular, we compare with the following baselines: (1) dreamfusion-IF (Poole et al., 2023), (2) magic3d-IF (Lin et al., 2023a), (3) text2mesh-IF (Tsalicoglou et al., 2023), (4) prolificdreamer (Wang et al., 2023c). Because these baselines either uses non-public diffusion models or has not yet released their source code by the time of this paper, the implementation in threestudio could be different from the original papers. For example, dreamfusion-IF, magic-3d-IF and text2mesh-IF uses DeepFloyd (dee) as their diffusion guidance while original ones use Imagen (Saharia et al., 2022) and eDiff-I (Balaji et al., 2022). Original dreamfusion uses Mip-NeRF 360 (Barron et al., 2022) as their 3D representation. But here all the methods (including ours) use the implicit-volume, i.e. multi-resolution hash-grid (Müller et al., 2022), from threestudio as its first stage base representation (except TextMesh which uses SDF). Although we are not able to compare the difference between these implementation details, we believe that the baselines here represent the best re-implementation we could find. To test the performance of our system as well as baselines comprehensively, we collected 40 prompts from different sources, including prompts from prior studies (Poole et al., 2023; Wang et al., 2023a), prompts that are composed based on the style of existing real 3D assets, and real user inputs from a 3D generation startup (lum). The results are shown in Fig. (6). Overall, we found that all of the baselines suffer from severe multi-view consistency issue. Among the three

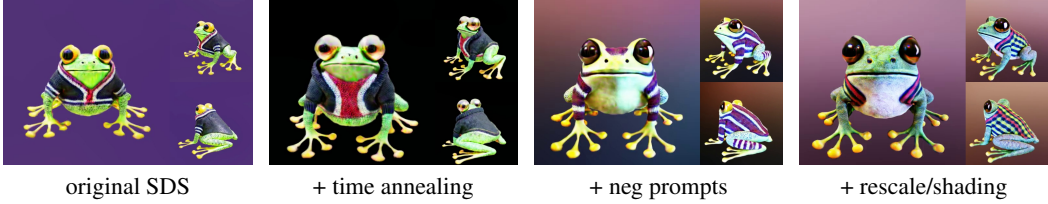


Figure 7: Effects of different techniques that we apply in multi-view SDS. The input text is "a DSLR photo of a frog wearing sweater".

DeepFloyd-based methods (Dreamfusion-IF, Magic3D-IF and TextMesh-IF), Magic3D performs the best by incorporating mesh representation and second stage refinement. However, it still cannot solve the multi-face problem. Prolificdreamer shows very good texture quality, where every view looks like a nice picture. But jointly they do not appear to be a reasonable 3D object. On the other side, the proposed method can generate high quality 3D assets in a much more stable way.

In Fig. (7), we show a comparison between the effects of different techniques that we applied in our multi-view score distillation. In general, adding time annealing helps to make the shape more complete. Adding negative prompts significantly improves the visual style, but could hurt the text-image correspondence. Adding the CFG rescale and shading further makes the texture color more natural.

To further validate the stability and quality of our model, we conduct a user study on the generated models from 40 prompts. Each user is given 5 rendered videos and its corresponding text input and is asked to select his/her preferred 3D model among all. 914 feedbacks from 38 users were collected from the study and the result is shown in Fig. (8). On average, 78% of users prefer our model over others. In other words, our model is preferred over the best of all baselines in most cases. We believe this is a strong proof of the robustness and quality of the proposed method. Please see the supplementary materials for more visual results.

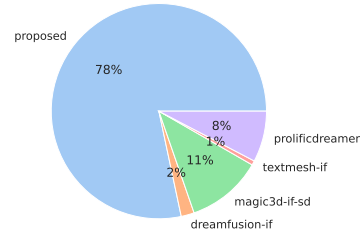


Figure 8: User study.

5.3 MULTI-VIEW DREAMBOOTH.

In Fig. (9), we compare 3D models generated from MVDream and DreamBooth3D (Raj et al., 2023). In the listed examples, we show that our results have higher quality with better object details such as the curly hair and fur texture on the dog. This is because during the NeRF training process with SDS loss, our MV DreamBooth diffusion models produce higher geometry consistency. We provide additional results in our project page and supplementary materials.

6 DISCUSSION AND CONCLUSION

Conclusion In this paper, we present the first multi-view diffusion model that is able to generate a set of multi-view images of an object/scene from any given text. By fine-tuning a pre-trained text-to-image diffusion model on a mixture of 3D rendered datasets and large scale text-to-image datasets, our model is able to maintain the generalizability of the base model while achieving multi-view consistent generation. With a comprehensive design exploration, we found that using a 3D self-attention with camera matrix embedding is sufficient to learn the multi-view consistency from training data. We show that the multi-view diffusion model can serve as a good 3D prior and can be applied to 3D generation via SDS, which leads to better stability and quality than current open-sourced 2D lifting methods. Finally, the multi-view diffusion model can also be trained under a few shot setting for personalized 3D generation (multi-view dreambooth).

Limitation We observe the following limitations of our current multi-view diffusion models. For the moment, the model can only generate images at a resolution of 256×256 , which is smaller than the 512×512 of the original stable diffusion. Also, the generalizability of the current model seems to be limited by the base model itself. For both aforementioned problems, we expect them to be solved

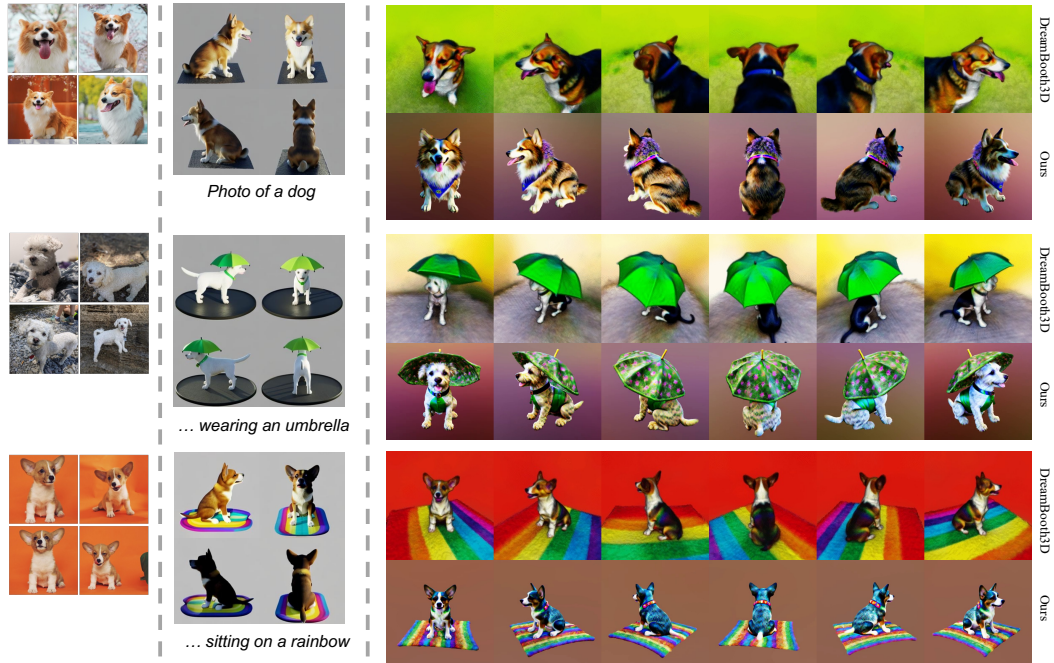


Figure 9: Illustration of MVDream DreamBooth Results. From the inputs, we show the generated multi-view images (MV Images) given a description prompt at bottom. On the right, we show comparison of NeRF rendered results from ours with that from DreamBooth3D (Raj et al., 2023). Notice ours handle better on the object details such as furry skin.

by increasing the dataset size and replacing the base model with a larger diffusion model, such as SDXL (SDX). Furthermore, we do observe that the generated styles (lighting, texture) of our model would tend to be similar to the rendered dataset, although it can be alleviated by adding more style text prompts, it also indicates that a more diverse and realistic rendering is necessary to learn a better multi-view diffusion model, which could be costly.

Societal Impacts The multi-view diffusion model proposed in this paper aims to facilitate the 3D generation task that widely demanded in gaming and media industry. We do note that it could be potentially applied to unexpected scenarios such as generating violent and sexual content by third-party fine-tuning. Therefore, we believe that the images/models synthesized using our approach should present itself as synthetic.

REFERENCES

- stable-diffusion-xl-base-1.0. <https://huggingface.co/stabilityai/stable-diffusion-xl-base-1.0>. Accessed: 2023-08-29. 12
- Sketchfab. <https://sketchfab.com/3d-models/popular>. Accessed: 2023-08-30. 1
- Deepfloyd. <https://huggingface.co/DeepFloyd>. Accessed: 2023-08-25. 10
- Luma.ai. <https://lumalabs.ai/dashboard/imagine>. Accessed: 2023-08-25. 10
- Stable diffusion image variation. <https://huggingface.co/spaces/lambdalabs/stable-diffusion-image-variations>. 3
- Stable diffusion. <https://github.com/CompVis/stable-diffusion>. Accessed: 2023-07-14. 3
- Threestudio project. <https://github.com/threestudio-project/threestudio>. Accessed: 2023-08-25. 7, 10

-
- Yogesh Balaji, Seungjun Nah, Xun Huang, Arash Vahdat, Jiaming Song, Karsten Kreis, Miika Aittala, Timo Aila, Samuli Laine, Bryan Catanzaro, et al. ediffi: Text-to-image diffusion models with an ensemble of expert denoisers. *arXiv:2211.01324*, 2022. 10
- Jonathan T. Barron, Ben Mildenhall, Dor Verbin, Pratul P. Srinivasan, and Peter Hedman. Mip-nerf 360: Unbounded anti-aliased neural radiance fields. *CVPR*, 2022. 10
- Andreas Blattmann, Robin Rombach, Huan Ling, Tim Dockhorn, Seung Wook Kim, Sanja Fidler, and Karsten Kreis. Align your latents: High-resolution video synthesis with latent diffusion models. In *CVPR*, 2023. 3, 4
- Eric R Chan, Connor Z Lin, Matthew A Chan, Koki Nagano, Boxiao Pan, Shalini De Mello, Orazio Gallo, Leonidas J Guibas, Jonathan Tremblay, Sameh Khamis, et al. Efficient geometry-aware 3d generative adversarial networks. In *CVPR*, 2022. 2
- Eric R. Chan, Koki Nagano, Matthew A. Chan, Alexander W. Bergman, Jeong Joon Park, Axel Levy, Miika Aittala, Shalini De Mello, Tero Karras, and Gordon Wetzstein. GeNVS: Generative novel view synthesis with 3D-aware diffusion models. In *arXiv*, 2023. 3
- Rui Chen, Yongwei Chen, Ningxin Jiao, and Kui Jia. Fantasia3d: Disentangling geometry and appearance for high-quality text-to-3d content creation. *arXiv:2303.13873*, 2023. 3
- Matt Deitke, Dustin Schwenk, Jordi Salvador, Luca Weihs, Oscar Michel, Eli VanderBilt, Ludwig Schmidt, Kiana Ehsani, Aniruddha Kembhavi, and Ali Farhadi. Objaverse: A universe of annotated 3d objects. In *CVPR*, 2023. 2, 7
- Yu Deng, Jiaolong Yang, Jianfeng Xiang, and Xin Tong. Gram: Generative radiance manifolds for 3d-aware image generation. In *CVPR*, pp. 10673–10683, 2022. 2
- Jun Gao, Tianchang Shen, Zian Wang, Wenzheng Chen, Kangxue Yin, Daiqing Li, Or Litany, Zan Gojcic, and Sanja Fidler. Get3d: A generative model of high quality 3d textured shapes learned from images. *NeurIPS*, 2022. 2
- Paul Henderson and Vittorio Ferrari. Learning single-image 3d reconstruction by generative modelling of shape, pose and shading. *International Journal of Computer Vision*, 2020. 2
- Paul Henderson, Vagia Tsiminaki, and Christoph H Lampert. Leveraging 2d data to learn textured 3d mesh generation. In *CVPR*, 2020. 2
- Martin Heusel, Hubert Ramsauer, Thomas Unterthiner, Bernhard Nessler, and Sepp Hochreiter. Gans trained by a two time-scale update rule converge to a local nash equilibrium. *NeurIPS*, 2017. 9
- Jonathan Ho, William Chan, Chitwan Saharia, Jay Whang, Ruiqi Gao, Alexey Gritsenko, Diederik P Kingma, Ben Poole, Mohammad Norouzi, David J Fleet, et al. Imagen video: High definition video generation with diffusion models. *arXiv:2210.02303*, 2022. 3, 4
- Yukun Huang, Jianan Wang, Yukai Shi, Xianbiao Qi, Zheng-Jun Zha, and Lei Zhang. Dreamtime: An improved optimization strategy for text-to-3d content creation. *arXiv:2306.12422*, 2023. 3
- Heewoo Jun and Alex Nichol. Shap-e: Generating conditional 3d implicit functions. *arXiv:2305.02463*, 2023. 2
- Animesh Karnewar, Andrea Vedaldi, David Novotny, and Niloy J Mitra. Holodiffusion: Training a 3d diffusion model using 2d images. In *CVPR*, 2023. 2
- Diederik P Kingma and Jimmy Ba. Adam: A method for stochastic optimization. In *ICLR*, 2014. 7
- Diederik P Kingma and Max Welling. Auto-encoding variational bayes. In *ICLR*, 2014. 2
- Chen-Hsuan Lin, Jun Gao, Luming Tang, Towaki Takikawa, Xiaohui Zeng, Xun Huang, Karsten Kreis, Sanja Fidler, Ming-Yu Liu, and Tsung-Yi Lin. Magic3d: High-resolution text-to-3d content creation. In *CVPR*, 2023a. 1, 3, 6, 7, 10
- Shanchuan Lin, Bingchen Liu, Jiashi Li, and Xiao Yang. Common diffusion noise schedules and sample steps are flawed. *arXiv:2305.08891*, 2023b. 6, 15

-
- Ruoshi Liu, Rundi Wu, Basile Van Hoorick, Pavel Tokmakov, Sergey Zakharov, and Carl Vondrick. Zero-1-to-3: Zero-shot one image to 3d object. *arXiv:2303.11328*, 2023. 3, 6
- Ben Mildenhall, Pratul P Srinivasan, Matthew Tancik, Jonathan T Barron, Ravi Ramamoorthi, and Ren Ng. Nerf: Representing scenes as neural radiance fields for view synthesis. In *ECCV*, 2021. 1, 3
- Thomas Müller, Alex Evans, Christoph Schied, and Alexander Keller. Instant neural graphics primitives with a multiresolution hash encoding. *ACM Trans. Graph.*, 2022. 10
- Thu Nguyen-Phuoc, Chuan Li, Lucas Theis, Christian Richardt, and Yong-Liang Yang. Hologan: Unsupervised learning of 3d representations from natural images. In *Proceedings of the IEEE/CVF International Conference on Computer Vision*, 2019. 2
- Thu H Nguyen-Phuoc, Christian Richardt, Long Mai, Yongliang Yang, and Niloy Mitra. Blockgan: Learning 3d object-aware scene representations from unlabelled images. *NeurIPS*, 2020. 2
- Alex Nichol, Heewoo Jun, Prafulla Dhariwal, Pamela Mishkin, and Mark Chen. Point-e: A system for generating 3d point clouds from complex prompts. *arXiv:2212.08751*, 2022. 2
- Michael Niemeyer and Andreas Geiger. Giraffe: Representing scenes as compositional generative neural feature fields. In *CVPR*, 2021. 2
- Ben Poole, Ajay Jain, Jonathan T. Barron, and Ben Mildenhall. Dreamfusion: Text-to-3d using 2d diffusion. In *ICLR*, 2023. 1, 3, 6, 10
- Alec Radford, Jong Wook Kim, Chris Hallacy, Aditya Ramesh, Gabriel Goh, Sandhini Agarwal, Girish Sastry, Amanda Askell, Pamela Mishkin, Jack Clark, et al. Learning transferable visual models from natural language supervision. In *ICML*, 2021. 9
- Amit Raj, Srinivas Kaza, Ben Poole, Michael Niemeyer, Nataniel Ruiz, Ben Mildenhall, Shiran Zada, Kfir Aberman, Michael Rubinstein, Jonathan Barron, et al. Dreambooth3d: Subject-driven text-to-3d generation. *arXiv:2303.13508*, 2023. 2, 3, 11, 12
- Robin Rombach, Andreas Blattmann, Dominik Lorenz, Patrick Esser, and Björn Ommer. High-resolution image synthesis with latent diffusion models. In *CVPR*, 2022. 3, 7
- Nataniel Ruiz, Yuanzhen Li, Varun Jampani, Yael Pritch, Michael Rubinstein, and Kfir Aberman. Dreambooth: Fine tuning text-to-image diffusion models for subject-driven generation. In *CVPR*, 2023. 2, 7
- Chitwan Saharia, William Chan, Saurabh Saxena, Lala Li, Jay Whang, Emily L Denton, Kamyar Ghasemipour, Raphael Gontijo Lopes, Burcu Karagol Ayan, Tim Salimans, et al. Photorealistic text-to-image diffusion models with deep language understanding. *NeurIPS*, 2022. 6, 10, 15
- Tim Salimans, Ian Goodfellow, Wojciech Zaremba, Vicki Cheung, Alec Radford, and Xi Chen. Improved techniques for training gans. *NeurIPS*, 2016. 9
- Christoph Schuhmann, Romain Beaumont, Richard Vencu, Cade Gordon, Ross Wightman, Mehdi Cherti, Theo Coombes, Aarush Katta, Clayton Mullis, Mitchell Wortsman, et al. Laion-5b: An open large-scale dataset for training next generation image-text models. *NeurIPS*, 2022. 6, 7
- J Ryan Shue, Eric Ryan Chan, Ryan Po, Zachary Anknor, Jiajun Wu, and Gordon Wetzstein. 3d neural field generation using triplane diffusion. In *CVPR*, 2023. 2
- Uriel Singer, Adam Polyak, Thomas Hayes, Xi Yin, Jie An, Songyang Zhang, Qiyuan Hu, Harry Yang, Oron Ashual, Oran Gafni, et al. Make-a-video: Text-to-video generation without text-video data. *arXiv:2209.14792*, 2022. 3, 4, 5
- Vincent Sitzmann, Michael Zollhöfer, and Gordon Wetzstein. Scene representation networks: Continuous 3d-structure-aware neural scene representations. *NeurIPS*, 32, 2019. 3
- Shitao Tang, Fuayng Zhang, Jiacheng Chen, Peng Wang, and Furukawa Yasutaka. Mvdifffusion: Enabling holistic multi-view image generation with correspondence-aware diffusion. *arXiv:2307.01097*, 2023. 3

- Christina Tsalicoglou, Fabian Manhardt, Alessio Tonioni, Michael Niemeyer, and Federico Tombari. Textmesh: Generation of realistic 3d meshes from text prompts. *arXiv:2304.12439*, 2023. 3, 10
- Haochen Wang, Xiaodan Du, Jiahao Li, Raymond A Yeh, and Greg Shakhnarovich. Score jacobian chaining: Lifting pretrained 2d diffusion models for 3d generation. In *CVPR*, 2023a. 3, 10
- Tengfei Wang, Bo Zhang, Ting Zhang, Shuyang Gu, Jianmin Bao, Tadas Baltrusaitis, Jingjing Shen, Dong Chen, Fang Wen, Qifeng Chen, et al. Rodin: A generative model for sculpting 3d digital avatars using diffusion. In *CVPR*, 2023b. 2
- Zhengyi Wang, Cheng Lu, Yikai Wang, Fan Bao, Chongxuan Li, Hang Su, and Jun Zhu. Prolificdreamer: High-fidelity and diverse text-to-3d generation with variational score distillation. *arXiv:2305.16213*, 2023c. 3, 10
- Daniel Watson, William Chan, Ricardo Martin-Brualla, Jonathan Ho, Andrea Tagliasacchi, and Mohammad Norouzi. Novel view synthesis with diffusion models. In *ICLR*, 2023. 2
- Chao-Yuan Wu, Justin Johnson, Jitendra Malik, Christoph Feichtenhofer, and Georgia Gkioxari. Multiview compressive coding for 3d reconstruction. In *CVPR*, 2023. 2
- Daquan Zhou, Weimin Wang, Hanshu Yan, Weiwei Lv, Yizhe Zhu, and Jiashi Feng. Magicvideo: Efficient video generation with latent diffusion models. *arXiv:2211.11018*, 2022. 3, 4
- Zhizhuo Zhou and Shubham Tulsiani. Sparsefusion: Distilling view-conditioned diffusion for 3d reconstruction. In *CVPR*, 2023. 3

A APPENDIX

A.1 \mathbf{x}_0 RECONSTRUCTION LOSS FOR SDS

The original SDS loss does not have an explicit form, instead it is defined as by its gradient:

$$\nabla_{\phi} \mathcal{L}_{SDS}(\theta, \mathbf{x} = g(\phi)) = \mathbb{E}_{t, \mathbf{c}, \epsilon} [w(t)(\epsilon_{\theta}(\mathbf{x}_t; y, \mathbf{c}, t) - \epsilon) \frac{\partial \mathbf{x}}{\partial \phi}] \quad (4)$$

where \mathbf{c} is the additional camera condition for our specific model, $\mathbf{x}_t = \alpha_t \mathbf{x} + \sigma_t \epsilon$ is the sampled noisy image, and $w(t)$ is a hyper-parameter that controls the loss weight at different time steps. α_t and σ_t are the signal and noise scale controlled by the noise schedule, where $\alpha_t^2 + \sigma_t^2 = 1$. Let us denote $\epsilon_{\theta}(\mathbf{x}_t; y, \mathbf{c}, t)$ as ϵ_{θ} for simplicity. Given estimated ϵ_{θ} predicted by the model, we can reversely estimate $\hat{\mathbf{x}}_0$ by:

$$\begin{aligned} \hat{\mathbf{x}}_0 &= \frac{\mathbf{x}_t - \sigma_t \epsilon_{\theta}}{\alpha_t} \\ &= \frac{\alpha_t \mathbf{x} + \sigma_t \epsilon - \sigma_t \epsilon_{\theta}}{\alpha_t} \\ &= \mathbf{x} + \frac{\sigma_t}{\alpha_t} (\epsilon - \epsilon_{\theta}) \end{aligned} \quad (5)$$

So for the reconstruction loss $\mathcal{L}_{SDS} = \mathbb{E}_{t, \mathbf{c}, \epsilon} [\|\hat{\mathbf{x}}_0 - \mathbf{x}\|_2^2]$, if we ignore $\frac{\partial \hat{\mathbf{x}}_0}{\partial \phi}$ like in SDS, its gradient is given by:

$$\begin{aligned} \nabla_{\phi} \mathcal{L}_{SDS}(\theta, \mathbf{x} = g(\phi)) &= \mathbb{E}_{t, \mathbf{c}, \epsilon} \left[2(\mathbf{x} - \hat{\mathbf{x}}_0) \frac{\partial \mathbf{x}}{\partial \phi} \right] \\ &= \mathbb{E}_{t, \mathbf{c}, \epsilon} \left[\frac{2\sigma_t}{\alpha_t} (\epsilon_{\theta} - \epsilon) \frac{\partial \mathbf{x}}{\partial \phi} \right], \end{aligned} \quad (6)$$

which is equivalent to the original SDS with $w(t) = \frac{2\sigma_t}{\alpha_t}$. Thus, we can further adjust the $\hat{\mathbf{x}}_0$ here with other tricks such as dynamic threshold (Saharia et al., 2022) or CFG rescale (Lin et al., 2023b).

A.2 ADDITIONAL RESULTS

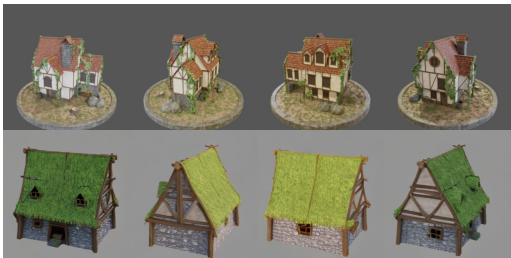
In Fig. (10), we show additional image generation results from our model using the prompts from the training dataet. In Fig. (11) and (12), we show additional comparison results of 3D generation using our method and baseline.



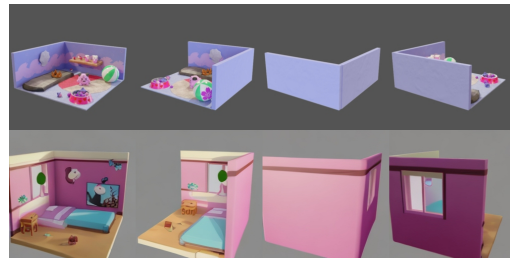
Zombie bust, terror, 123dsculpt, bust, zombie



BattleTech Zeus with a sword!, tabletop, miniature, battletech, miniatures, wargames



Medieval House, grass, medieval, vines, farm, middle-age, medieval-house, stone, house, home, wood, medieval-decor



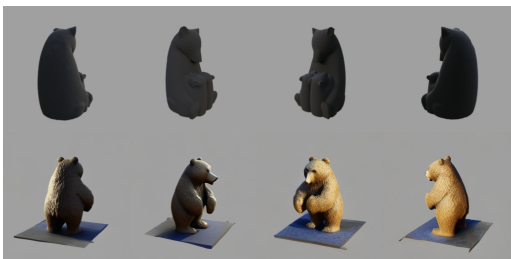
Isometric Slowpoke Themed Bedroom, fanart, pokemon, bedroom, assignment, isometric, pokemon3d, isometric-room, room-low-poly



Old Boot (Left), cloth, boot, old, substancepainter, substance, character



Old Treasure Chest, chest, vintage, treasure, old, substancepainter, substance



UCSF's Bear Mascot Sculpture, bear, library, sanfrancisco, photogramm, ucsf, kalmanovitz, bufano



DSLR Camera, photography, dslr, camera, noobie, box-modeling, maya

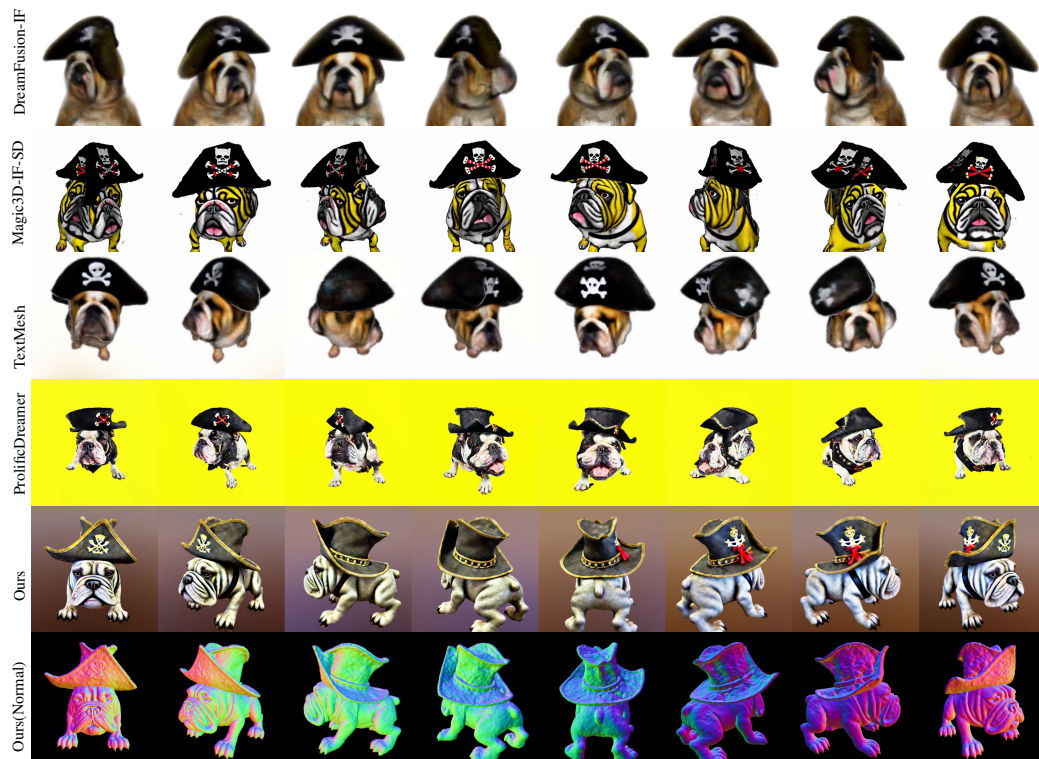


"Legolas" Custom Outfit, custom, free-model, fortnite-



Digital Wristwatch, wristwatch, timepiece, digital, watch

Figure 10: Example images generated by our multiview diffusion model using prompts in training set. In each example, the top and bottom row are the training and generated images, respectively.

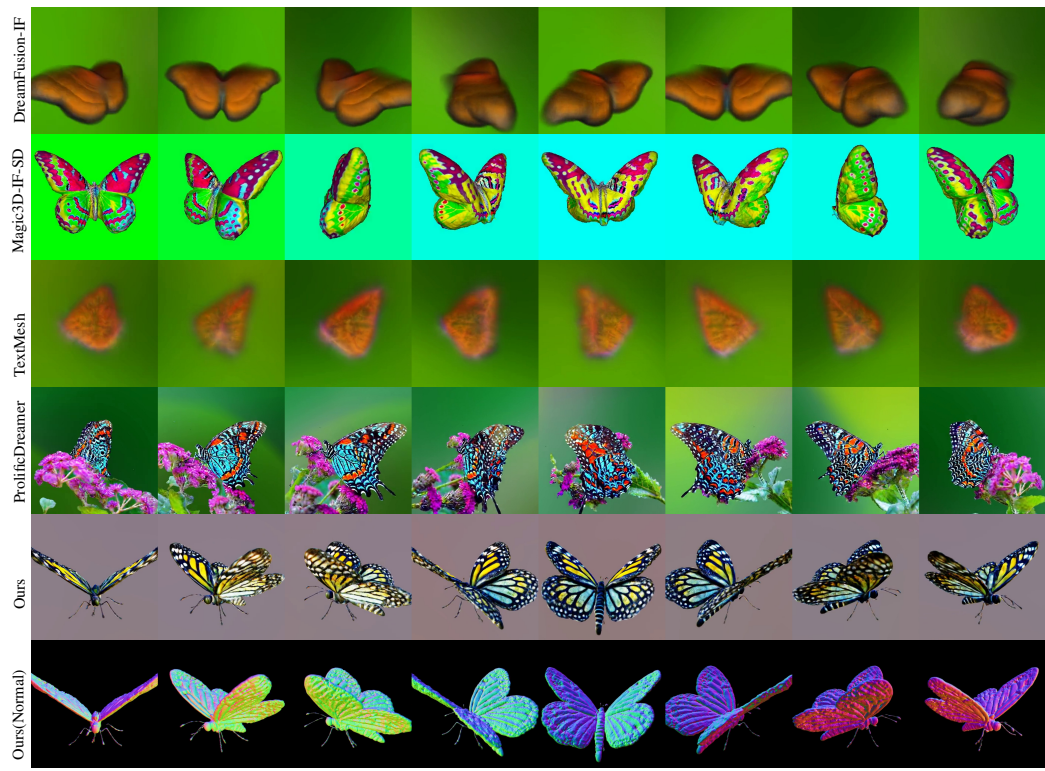


A bulldog wearing a black pirate hat

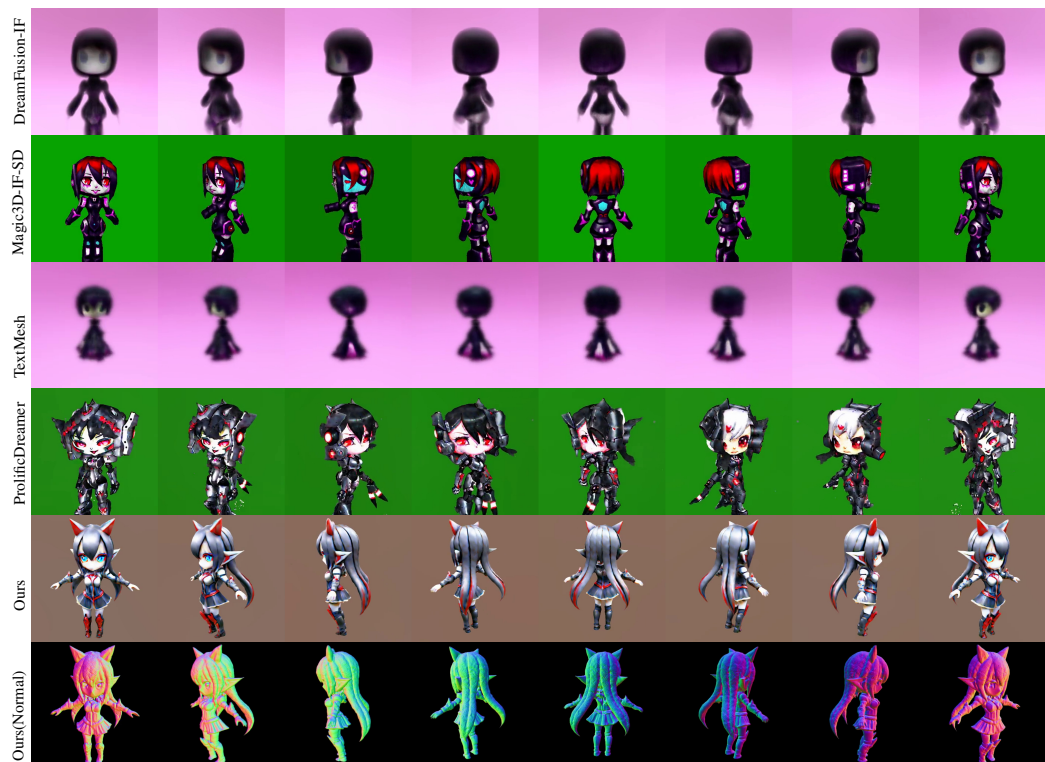


Viking axe, fantasy, weapon, blender, 8k, HD

Figure 11: Comparison of 3D generation between baselines and our method.



beautiful, intricate butterfly



mecha vampire girl chibi

Figure 12: Comparison of 3D generation between baselines and our method.